Available online at www.sciencedirect.com
SCIENCE DIRECT
Journal of Molecular Structure 744–747 (2005) 535–540
Journal of MOLECULAR STRUCTURE
www.elsevier.com/locate/molstruc

Synthesis and characterisation of bismuth(III) vanadate

M. Gotić[a,*], S. Musić[a], M. Ivanda[a], M. Šoufek[b], S. Popović[c]

[a]*Ruđer Bošković Institute, P.O. Box 180, HR-10002 Zagreb, Croatia*
[b]*Department of Mineralogy and Petrology, Croatian Natural History Museum, Zagreb, Croatia*
[c]*Department of Physics, Faculty of Science, University of Zagreb, P.O. Box 331, HR-10002 Zagreb, Croatia*

Received 6 September 2004; accepted 11 October 2004
Available online 11 January 2005

Abstract

Modified hydrothermal and 'wet' precipitation routes at room temperature were employed to synthesise pure monoclinic $BiVO_4$ powders of varying particle morphologies. Monoclinic $BiVO_4$ powder was also prepared by a solid-state reaction at 700°C. Depending on the synthesis conditions, the colour of $BiVO_4$ varies from inhomogeneously yellow–brown to homogeneously and intensive lemon yellow. $BiVO_4$ prepared by solid-state reaction consisted of large compact particles about 15 μm in size and of irregular shape. At higher magnification, the formation of domains with smooth terrace-like surfaces was observed. These domains ended with well-defined walls, and the edges of these walls were relatively very sharp. $BiVO_4$ synthesised by the hydrothermal and an aqueous process at RT consisted of smaller particles (0.3–1.2 μm) and of much bigger regular crystals with a well-defined crystal habit. A continuous shift of the most intense Raman band to lower wavenumbers reveals that the average short range symmetry of the VO_4 tetrahedra becomes more regular. The values of FWHM for the same Raman band increase from sample prepared by solid-state reaction to sample obtained at RT. The Raman results suggested that a sample prepared at high temperature consisted of less symmetric VO_4 tetrahedra than samples prepared at low temperature and that the high-temperature sample showed better crystallinity with less defects than the samples prepared by an aqueous process under mild conditions. FT-IR spectra showed main features typical of the vanadates of other metal(3+) cations. However, the position of IR bands recorded for $BiVO_4$ depended on the synthesis route.

Keywords: $BiVO_4$; Bismuth vanadate; Hydrothermal synthesis; 'Wet' precipitation; Solid state; Raman; FT-IR; Electron microscopy; XRD

1. Introduction

Bismuth(III) vanadate ($BiVO_4$) shows ferroelastic and pyrooptical properties. $BiVO_4$ is a possible candidate for use as electrolyte or cathode material in solid oxide fuel cells. In addition, $BiVO_4$ shows catalytic and photocatalytic properties. It is commonly used as catalyst in oxidative dehydrogenation, e.g. converting ethyl benzene to styrene. $BiVO_4$ is a very good photocatalyst, as shown by Kudo et al. [1–3], who reported a high activity for the O_2 evolution from an aqueous silver nitrate solution under visible light irradiation. $BiVO_4$ is also a commercially available high-performance pigment that could eliminate the more expensive and less stable organic pigment. It is classified as non-toxic and could replace toxic pigments such as cadmium and lead-based paints. However, it has been proven difficult to control the pigmentary colours of $BiVO_4$. Colour intensity depends on many factors including phase composition, stoichiometry, particle size and morphology. Also, photophysical and photocatalytic properties of $BiVO_4$ are strongly influenced by the way of preparation and its crystal structure. For example, tetragonal structure of $BiVO_4$ absorbs in the ultraviolet region (band gap 2.9 eV), whereas monoclinic structure of $BiVO_4$ with a 2.4 eV band gap has a characteristic visible light absorption in addition to the UV band [2]. The photocatalytic activities of tetragonal and monoclinic $BiVO_4$ differ markedly. Also, the photocatalytic activity of the monoclinic $BiVO_4$ prepared by the aqueous process at room temperature was much higher than that of monoclinic $BiVO_4$ prepared by a conventional solid-state reaction even in the same crystal structure.

* Corresponding author. Tel.: +385 1 456 1123.
E-mail address: gotic@irb.hr (M. Gotić).

0022-2860/$ - see front matter © 2004 Elsevier B.V. All rights reserved.
doi:10.1016/j.molstruc.2004.10.075

Three main crystal forms of $BiVO_4$ are known; tetragonal (zircon-type structure), monoclinic (distorted scheelite structure, fergusonite structure) and tetragonal scheelite structure (high-temperature phase). The phase transition between monoclinic scheelite structure and tetragonal scheelite structure of $BiVO_4$ reversibly occurs at about 255 °C (ferroelastic to paraelastic transition), whereas the irreversible transition from tetragonal zircon-type structure to monoclinic $BiVO_4$ occurs after heat treatment at 400–500 °C and cooling to room temperature.

Generally, monoclinic $BiVO_4$ is usually obtained by the high-temperature process, whereas tetragonal $BiVO_4$ with a zircon-type structure is prepared in aqueous media by the low-temperature process. Bhattacharya et al. [4] reported a co-precipitation method from a $Bi(NO_3)_3$ nitric acid solution and an aqueous NH_4VO_3 at room temperature to produce fully crystalline zircon-type tetragonal $BiVO_4$. Hirota et al. [5] synthesised monoclinic $BiVO_4$ by the hydrolysis of bismuth and vanadyl double alkoxide (sol–gel method). Monoclinic $BiVO_4$ powders were also prepared by a mild hydrothermal method (140–200 °C) using an aqueous solution of bismuth nitrate and two different vanadium sources (V_2O_5 and $NaVO_3$) [6]. The preparation of $BiVO_4$ as a monolayer on silica surfaces [7] or as a thin film on glass substrate obtained by the metalorganic decomposition technique has also been reported [8]. Wood and Glasser [9] prepared the pigmentary grade $BiVO_4$ by precipitation from an aqueous solution. Depending on the respective precipitation condition, either tetragonal or monoclinic structured phase were obtained.

In this work, we present a modified hydrothermal and RT synthesis routes used to obtain monoclinic $BiVO_4$ powders of various particle morphologies. Instead of the conventional inorganic alkali, in the present preparation of $BiVO_4$ a strong organic alkali, tetramethylammonium hydroxide (TMAH) capable of reaching pH values near ~14 in aqueous medium, was used. In a previous work, this organic alkali was employed in the synthesis of several metallic oxide such as Fe_2O_3, ZnO and RuO_2 [10–12]. Synthesis of monoclinic $BiVO_4$ powder was also performed starting from the highly acid aqueous solution under hydrothermal condition. For comparison, monoclinic scheelite $BiVO_4$ powder was also prepared by a solid-state reaction at 700°C. Bismuth vanadate powders were characterised by using XRD, Raman, FT-IR and TEM/SEM techniques.

2. Experimental

$Bi(NO_3)_3 \cdot 5H_2O$ (p.a., Kemika), NH_4VO_3 (p.a., Merck), tetramethylammonium hydroxide, TMAH, $(CH_3)_4NOH$, 25% (w/w) aqueous solution, electronic grade, 99.999% (metal basis) (Alfa Aeser®) and doubly distilled water were used. Samples were synthesised under the experimental conditions summarised in Table 1.

Sample BiV-1 was synthesised using solid-state reaction by mixing stoichiometric amounts of $Bi(NO_3)_3 \cdot 5H_2O$ and NH_4VO_3. During the mixing, the white colour of powders changes immediately to intensive orange-yellow colour. Powders were then dried for 24 h at 120°C to reduce foaming during calcination and to evaporate physical adsorbed water and partially decompose crystal water. Samples were then again homogenised and calcined for 8 h at 700°C.

Sample BiV-2 was synthesised using a hydrothermal route. Twenty milliliters of 4 M HNO_3 was added to 0.03 mol of $Bi(NO_3)_3 \cdot 5H_2O$, then stirred for 2 h at RT in a closed flask. A clear (homogeneous) solution was obtained. Separately, 20 ml of 25% (w/w) aqueous solution of TMAH was added to 0.03 mol of NH_4VO_3 and stirred for 2 h in a closed plastic bottle. Ammonium vanadate was also fully dissolved in an aqueous solution of TMAH. These two clear solutions were mixed, then stirred at RT for additional 30 min. The solution thus obtained was quantitatively transferred to a 50 ml Teflon-lined stainless autoclave, sealed and allowed to heat at 170°C for 130 h. The precipitate formed was isolated by centrifugation, washed several times with doubly distilled water and dried in a laboratory oven for 24 h at 60°C.

Table 1
Experimental conditions for the preparation of crystalline $BiVO_4$ powder samples

Sample	Amount of $Bi(NO_3)_3 \cdot 5H_2O$	Amount of NH_4VO_3	Experimental conditions	Autoclaving at 170 °C	Calcination
BiV-1	0.015 mol	0.015 mol	Ground in agate mortar at RT, heated for 24 h at 120°C, ground again	–	8 h at 700°C
BiV-2	0.03 mol in 20 ml of 4 M HNO_3 (homogeneous solution)	0.03 mol in 20 ml of 25% (w/w) aqueous solution of TMAH (homogeneous solution)	Each precursor stirred separately for 2 h at RT, then mixed and stirred for 30 min at RT	130 h	–
BiV-3	0.03 mol in 20 ml of 4 M HNO_3 (homogeneous solution)	0.03 mol in 20 ml of Re H_2O (dispersion)	Each precursor stirred separately for 2 h at RT, then mixed and stirred for 30 min at RT	120 h	–
BiV-4	0.03 mol in 20 ml of 25% (w/w) aqueous solution of TMAH (dispersion)	0.03 mol in 20 ml of 4 M HNO_3 (gelatinous-heterogeneous solution)	Each precursor stirred separately for 4 h, then mixed and stirred for 11 days at RT	–	–

Fig. 1. Photos of the synthesised $BiVO_4$ powders. Experimental procedures for the synthesis of these samples are summarised in Table 1. Depending on the synthesis conditions, the colour of $BiVO_4$ varies from inhomogeneously yellow-brown (sample BiV-1) to homogeneously and intensive lemon yellow (BiV-4).

Sample BiV-3 was synthesised using hydrothermal route under highly acid conditions. Bismuth salt was dissolved in 4 M HNO_3, while vanadium salts in doubly distilled water gave an aqueous dispersion. After mixing and stirring, the dispersion was transferred to the autoclave and heated at 170°C for 120 h. Precipitate was isolated by centrifugation and dried at 60°C for 24 h.

BiV-4 was synthesised using an aqueous process at RT. Bismuth salt gave a dispersion in TMAH, while vanadium salts in 4 M HNO_3 gave a gelatinous aqueous dispersion. Dispersions were mixed and stirred in a closed plastic bottle for 11 days. The precipitate formed was isolated in the same procedure as for samples BiV-2 and BiV-3. Fig. 1 shows the photos of the synthesised $BiVO_4$ powders.

X-ray powder diffraction (XRD) patterns were recorded in the region of $2\theta = 5$–$120°$ with a step scan of 1.1°/min at RT using a Philips counter diffractometer, model PW 3710 (Cu Kα radiation, graphite monochromator, proportional counter).

The Raman scattering experiments were performed using a standard instrumental technique. A Coherent Innova-100 laser with $\lambda = 514.5$ nm served as the excitation source and the scattered light was analyzed with a DILOR Z-24 Raman spectrometer.

The FT-IR spectra were recorded at room temperature using a Perkin–Elmer spectrometer (model 2000). The Infrared Data Manager (IRDM) program, supplied by Perkin–Elmer, was used to process the spectra. The FT-IR spectra of the samples pressed into KBr pellets were collected in the wave number range of 4000–400 cm^{-1} (mid-IR region) using the KBr beam splitter.

Transmission electron microscopy (TEM) was performed with an EM-10 Opton electron microscope.

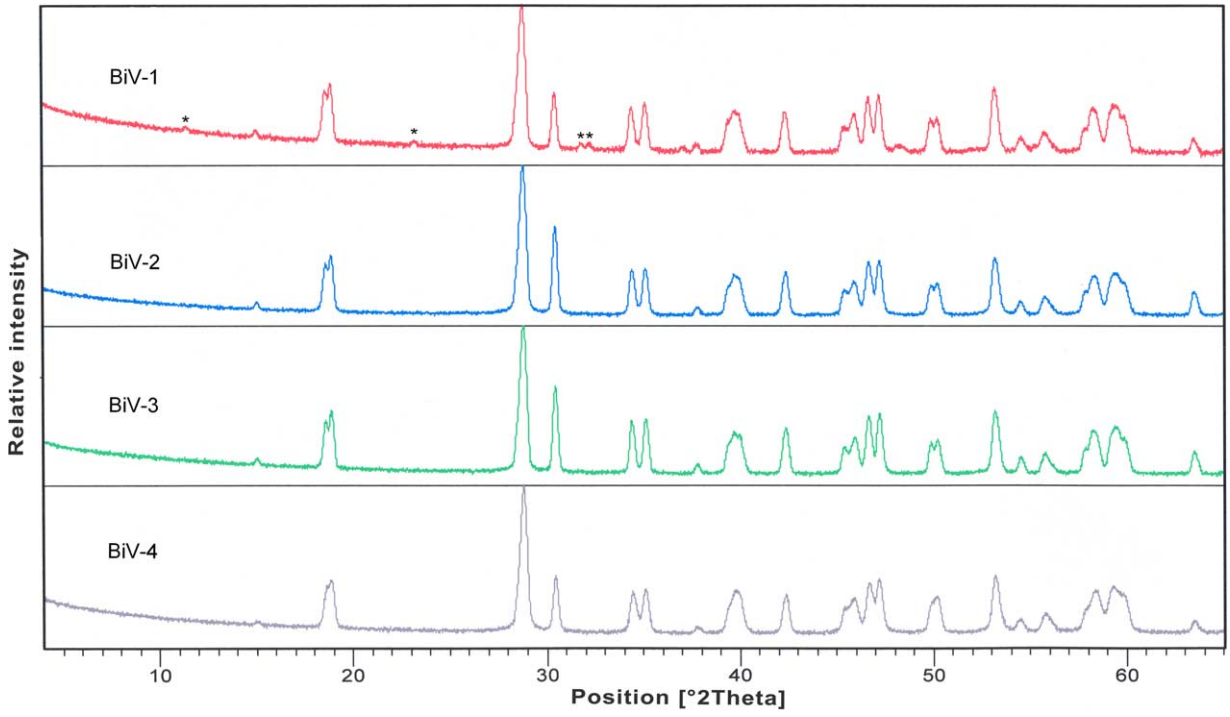

Fig. 2. Characteristic part of the X-ray powder diffraction patterns of samples BiV-1 to BiV-4. These patterns show an excellent match with the published JCPDS data (JCPDS file No.: 14-0688) for monoclinic $BiVO_4$. Sample BiV-1 contains a small amount of unidentified impurities (denoted by asterisks). These XRD maximums of very small intensity are in the positions $2\theta = 11.5$, 23.3, 31.8 and 32.3° (Cu Kα radiation) and do not belong to the $BiVO_4$ phase.

Scanning electron microscopy (SEM) was performed using a Field emission JEOL instrument, model JSM-6500, with a maximum voltage of up to 3 kV and using a TESCAN instrument, model SEM VEGA TS 5136, with a maximum voltage of up to 30 kV. Samples were prepared by placing powder onto a conductive graphite strip without making a gold coating.

3. Results and discussion

Fig. 2 shows the characteristic part of the X-ray powder diffraction patterns of samples BiV-1 to BiV-4. All these samples contained monoclinic $BiVO_4$ identified according to diffraction data in ICDD Powder Diffraction File (PDF) [13], e.g. card No. 83-1700, 83-1698, 14-0688 (monoclinic symmetry, space group $I2/a$, unit-cell parameters $a=5.195$, $b=11.701$, $c=5.092$ Å, $\beta=90.38°$, mineral name: clino-bisvanite). Diffraction lines of $BiVO_4$ were rather sharp for all investigated samples. XRD patterns of sample BiV-1, prepared by solid-state reaction, also contained traces of unidentified impurity (denoted by asterisk). Samples BIV-2, BiV-3 and BiV-4 contained monoclinic $BiVO_4$ as a single phase.

Fig. 3 shows FE SEM micrographs of sample BiV-1. This sample is of inhomogeneously yellow-brown colour containing bright and dark grains (Fig. 1). However, in spite of these macroscopic inhomogeneities, the particle surface on the micrometer level is homogeneous and relatively very smooth as shown in Fig. 3. At low magnification (Fig. 3a), large compact particles (about 10 μm in size) of irregular shape are visible. There is a negligible quantity of small irregular particles adhering to the large particles. At higher magnification, a new inside into the surface of these particles is visible. The formation of domains with smooth terrace-like surfaces was observed. These domains ended with well-defined walls, the edges of which were relatively very sharp.

Samples prepared by the aqueous routes consist of much smaller particles with significantly differing morphologies. Fig. 4 shows SEM micrographs of samples BiV-2 (a) and BiV-3 (b). Sample BiV-2 consists of smaller irregular particles organised in larger aggregates and of bigger particles with well-defined edges and planes. Sample BiV-3

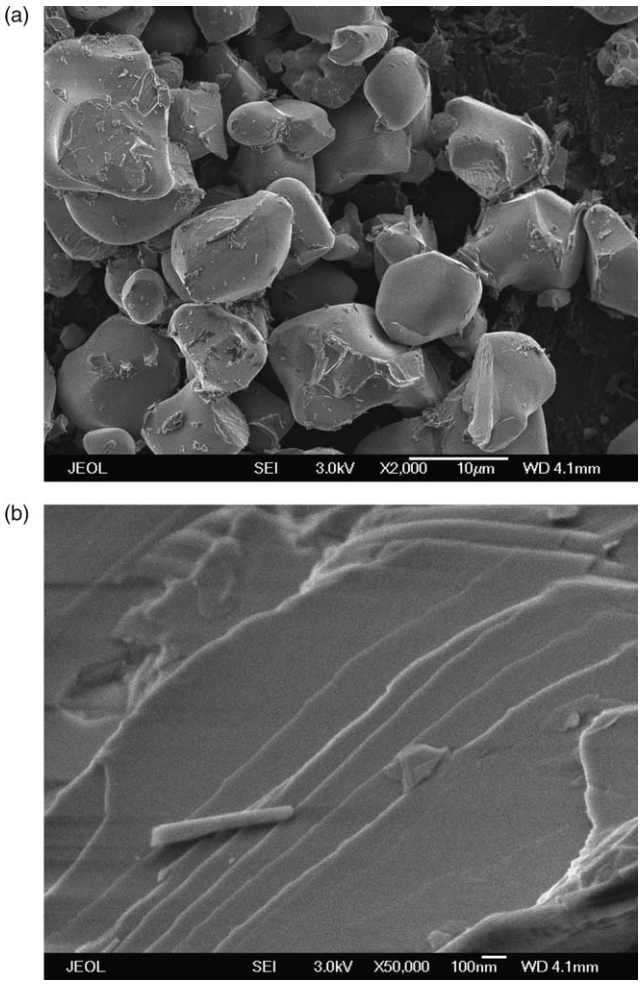

Fig. 3. FE SEM photographs of sample BiV-1 at (a) lower magnification and (b) at higher magnifications.

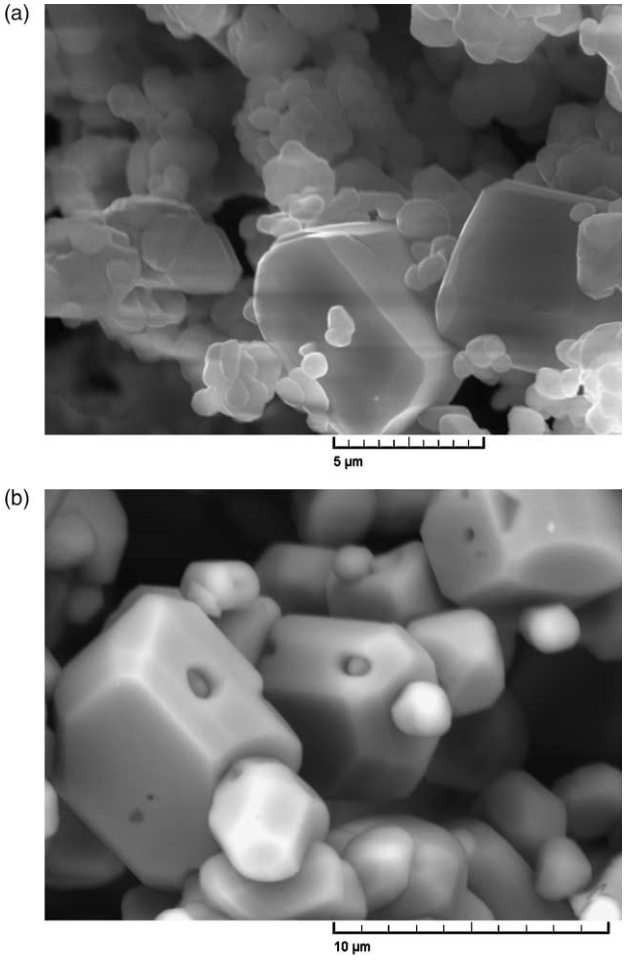

Fig. 4. SEM photographs of sample BiV-2 (a) and sample BiV-3 (b).

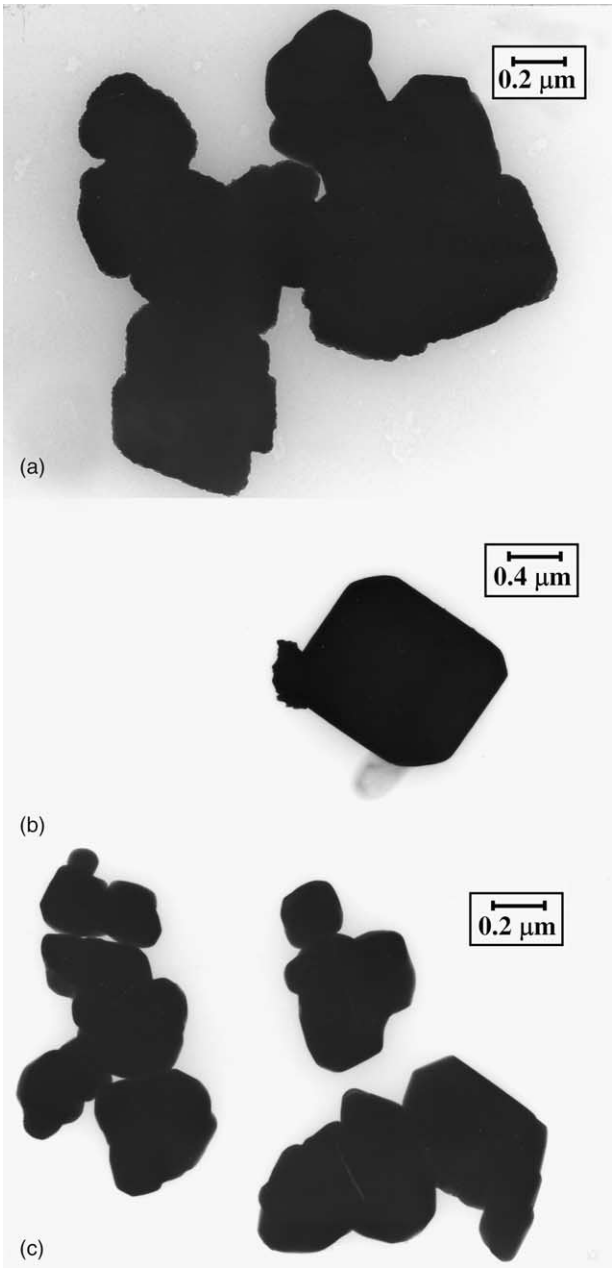

Fig. 5. TEM micrographs of sample BiV-2 (a), BiV-3 (b) and BiV-4 (c).

consists of even more regular particles. In this sample, large particles (about 5 μm in size) of well developed crystal habit are visible. Smaller particles also have developed edges and planes, but to a lesser extent than the bigger ones.

Fig. 5 shows the transmission electron micrographs of samples BiV-2 (a), BiV-3 (b) and BiV-4 (c). One can see that sample BiV-3 consists of the biggest and most regular particles, whereas sample BiV-4 consists of the smallest particles organised in relatively small aggregates.

Fig. 6 shows Raman spectra of the samples BiV-1 to BiV-4. The positions of assigned Raman bands are given in Table 2. The Raman spectra of crystalline $BiVO_4$ reflect the structure of one type of VO_4 tetrahedron that consists of two

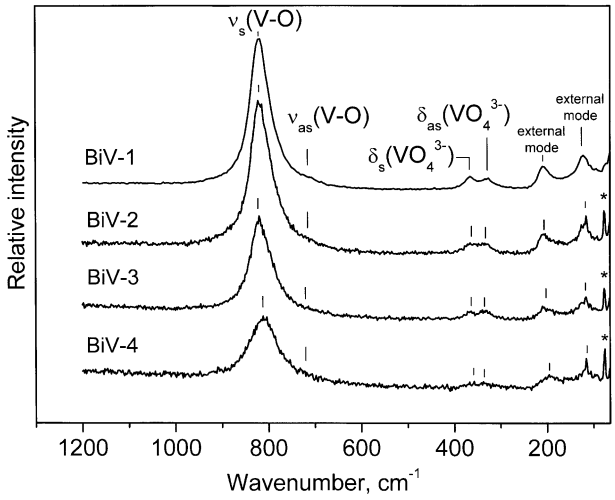

Fig. 6. Raman spectra of the samples BiV-1 to BiV-4. The positions of assigned Raman bands are given in Table 2. The sharp Raman bands at low wavenumbers denoted by asterisks belong to parasite lines.

sets of V–O bonds. In accordance with the interpretation of Hardcastle et al. [14], the most intense Raman band at about 818 cm^{-1} is assigned to the symmetric V–O stretching mode (A_g symmetry), the weak shoulder at about 712 cm^{-1} is assigned to antisymmetric V–O stretch (B_g symmetry), the symmetric (A_g) and antisymmetric (B_g) bending modes are at 365 and about 330 cm^{-1}, respectively, and external modes (rotation/translation) occur at 207 and 121 cm^{-1}. The positions of assigned Raman bands shown in Fig. 6 are reported in Table 2. The positions and the full width at half-maximum (FWHM) for the most intense Raman band at about 818 cm^{-1} were determined by the fitting to the Lorentzian peak function. A continuous shift of this Raman band to lower wavenumbers, from 818.5 to 812.4 cm^{-1} (Table 2), reveals that the average short-range symmetry of

Table 2
Assignations and Raman band positions for the Raman spectra of samples BiV-1 to BiV-4 shown in Fig. 3

Assignation	Sample			
	BiV-1 position of Raman band (cm^{-1})	BiV-2 position of Raman band (cm^{-1})	BiV-3 position of Raman band (cm^{-1})	BiV-4 position of Raman band (cm^{-1})
ν_s(V–O) (FWHM)	818.5 (50.0)	817.1 (53.2)	817.7 (57)	812.4 (76)
ν_{as}(V–O)	712	716	722	725
$\delta_s VO_4^{3-}$	365	365	365	362
$\delta_{as} VO_4^{3-}$	330	334	335	336
External mode	207	208	203	196
External mode	121	117	119	117

The position and the full width at half-maximum (FWHM) of the most intense band at about 818 cm^{-1} were determined by fitting on Lorentzian peak function.

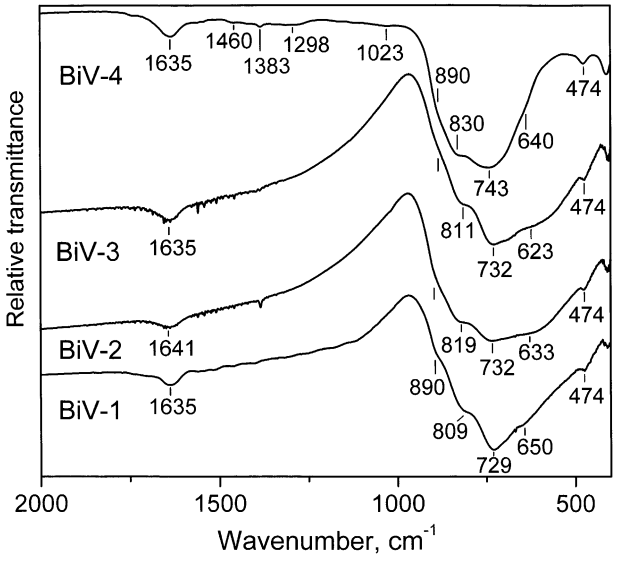

Fig. 7. FT-IR spectra of samples BiV-1 to BiV-4, recorded at RT.

the VO_4 tetrahedra becomes more regular [14]. On the contrary, the values of FWHM increase from sample BiV-1 prepared by solid-state reaction to sample BiV-4 obtained at RT. These Raman results are not in contradiction, because the Raman band positions are very sensitive to the short-range order, whereas the Raman widths are more sensitive to the degree of crystallinity, defects and disorders, particle size and/or aggregation of particles. Therefore, the Raman results imply that; (i) sample prepared at high temperature consisted of less symmetric VO_4 tetrahedra than samples prepared at low temperature, and (ii) a high-temperature sample was of better crystallinity and contained lesser defects than the samples prepared by an aqueous process under mild conditions.

Fig. 7 shows FT-IR spectra of samples BiV-1 to BiV-4, recorded at RT. The spectrum of sample BiV-1 is characterised by a very broad and strong IR band at 729 cm^{-1} with shoulders at 890, 809 and 650 cm^{-1}. A weak and intense IR band at 474 cm^{-1} is also visible. The IR band at 729 cm^{-1} observed for sample BiV-1 shifted to 743 cm^{-1} for sample BiV-4, whereas the band at 809 cm^{-1} shifted to 830 cm^{-1} for the same series of samples. The IR band at $\sim$1635 cm^{-1} corresponds to bending vibrations of adsorbed H_2O molecules. These FT-IR spectra can be related to the corresponding spectra of some other metal vanadates (MVO_4). For example, Yamaguchi et al. [15] prepared YVO_4 by the sol–gel procedure and the IR spectrum of this compound showed vibrations $\nu_1VO_4^{3}$ at 870 cm^{-1}, $\nu_3VO_4^{3-}$ at 820 cm^{-1}, $\nu_4VO_4^{3-}$ at 430 cm^{-1} and $\nu_2VO_4^{3-}$ at 350 cm^{-1}. Baran and Aymonino [16] observed, in the IR spectrum of $LaVO_4$, the vibration $\nu_4VO_4^{3-}$ at 432 cm^{-1}. These authors [17] also recorded $\nu_4VO_4^{3-}$ vibration for $CeVO_4$ at 442 cm^{-1}, for $PrVO_4$ at 441 cm^{-1}, for $NdVO_4$ at 443 cm^{-1}, for $SmVO_4$ at 445 cm^{-1}, for $EuVO_4$ at 443 cm^{-1} and for $GdVO_4$ at 448 cm^{-1}. In the present case, (VO_4^{3-}) vibration is recorded at 474 cm^{-1}. Near to that value, the corresponding $\nu_4VO_4^{3-}$ vibration was positioned for $LaVO_4$ crystallised in lead vanadate glasses containing La^{3+} ions [18]. The IR bands of very small intensities at 1460, 1383, 1298 and 1023 in sample BiV-4 correspond to the traces of organic impurity adsorbed on the surface of this sample.

References

[1] A. Kudo, K. Ueda, H. Kato, I. Mikami, Catal. Lett. 53 (1998) 229.
[2] A. Kudo, K. Omori, H. Kato, J. Am. Chem. Soc. 121 (1999) 11459.
[3] S. Tokunaga, H. Kato, A. Kudo, Chem. Mater. 13 (2001) 4624.
[4] A.K. Bhattacharya, K.K. Mallick, A. Hartridge, Mater. Lett. 30 (1997) 7.
[5] K. Hirota, G. Komatsu, M. Yamashita, H. Takemura, O. Yamaguchi, Mater. Res. Bull. 27 (1992) 823.
[6] J.B. Liu, H. Wang, S. Wang, H. Yan, Mater. Sci. Eng. B104 (2003) 36.
[7] V.P. Tolstoy, E.V. Tolstobrov, Solid State Ionics 151 (2002) 165.
[8] A. Galembeck, O.L. Alves, Thin Solid Films 365 (2000) 90.
[9] P. Wood, F.P. Glasser, Ceram. Int. 30 (2004) 875.
[10] S. Musić, I. Czakó-Nagy, I. Salaj-Obelić, N. Ljubešić, Mater. Lett. 32 (1997) 301.
[11] S. Musić, S. Popović, M. Maljković, Đ. Dragčević, J. Alloys Compd. 347 (2002) 324.
[12] S. Musić, S. Popović, M. Maljković, K. Furić, A. Gajović, Mater. Lett. 56 (2002) 806.
[13] International Centre for Diffraction Data, Joint Committee on Powder Diffraction Standards, Powder Diffraction file, 1601 Park Lane, Swarthmore, PA 19081, USA.
[14] F.D. Hardcastle, I.E. Wachs, H. Eckert, D.A. Jefferson, J. Solid State Chem. 90 (1991) 194.
[15] O. Yamaguchi, Y. Mukaida, H. Shigeta, H. Takemura, M. Yamashita, Mater. Lett. 7 (1988) 1558.
[16] E.J. Baran, P.J. Aymonino, Z. Anorg. Allg. Chem. 383 (1971) 220.
[17] E.J. Baran, P.J. Aymonino, Z. Anorg. Allg. Chem. 383 (1971) 226.
[18] S. Musić, M. Gotić, S. Popović, K. Furić, V. Mohaček, J. Mater. Sci. 29 (1994) 1227.